Available online at www.sciencedirect.com

ScienceDirect

www.elsevier.com/locate/jes

JES JOURNAL OF ENVIRONMENTAL SCIENCES

www.jesc.ac.cn

Research Article

Selenium deficiency exacerbates ROS/ER stress mediated pyroptosis and ferroptosis induced by bisphenol A in chickens thymus

Kun Wang[1], *Xu Shi*[1], *Hongjin Lin*[1], *Tong Xu*[1,*], *Shiwen Xu*[1,2,*]

[1] *College of Veterinary Medicine, Northeast Agricultural University, Harbin 150030, China*
[2] *Key Laboratory of the Provincial Education Department of Heilongjiang for Common Animal Disease Prevention and Treatment, China*

ARTICLE INFO

Article history:
Received 19 October 2023
Revised 10 January 2024
Accepted 10 January 2024
Available online 18 January 2024

Keywords:
Bisphenol A
Selenium deficiency
ROS/ER stress
Pyroptosis
Ferroptosis
Thymic injury

ABSTRACT

Bisphenol A (BPA) is an industrial pollutant that can cause immune impairment. Selenium acts as an antioxidant, as selenium deficiency often accompanies oxidative stress, resulting in organ damage. This study is the first to demonstrate that BPA and/or selenium deficiency induce pyroptosis and ferroptosis-mediated thymic injury in chicken and chicken lymphoma cell (MDCC-MSB-1) via oxidative stress-induced endoplasmic reticulum (ER) stress. We established a broiler chicken model of BPA and/or selenium deficiency exposure and collected thymus samples as research subjects after 42 days. The results demonstrated that BPA or selenium deficiency led to a decrease in antioxidant enzyme activities (T-AOC, CAT, and GSH-Px), accumulation of peroxides (H_2O_2 and MDA), significant upregulation of ER stress-related markers (GRP78, IER 1, PERK, EIF-2α, ATF4, and CHOP), a significant increase in iron ion levels, significant upregulation of pyroptosis-related gene (NLRP3, ASC, Caspase1, GSDMD, IL-18 and IL-1β), significantly increase ferroptosis-related genes (TFRC, COX2) and downregulate GPX4, HO-1, FTH, NADPH. In vitro experiments conducted in MDCC-MSB-1 cells confirmed the results, demonstrating that the addition of antioxidant (NAC), ER stress inhibitor (TUDCA) and pyroptosis inhibitor (Vx765) alleviated oxidative stress, endoplasmic reticulum stress, pyroptosis, and ferroptosis. Overall, this study concludes that the combined effects of oxidative stress and ER stress mediate pyroptosis and ferroptosis in chicken thymus induced by BPA exposure and selenium deficiency.

Introduction

Bisphenol A (BPA) is a commonly encountered organic compound in industrial settings, often utilized in the synthesis of production such as polycarbonate (PC) and epoxy resins (Rochester, 2013). Extensive research has demonstrated the widespread presence of BPA in our living environment, with the highest recorded residual concentration in air reaching 2454 pg/m^3 (Graziani et al., 2019). Concerningly, numerous studies have indicated that BPA poses a significant threat to human health primarily through dietary exposure.

* Corresponding authors.
E-mails: tongxu@neau.edu.cn (T. Xu), shiwenxu@neau.edu.cn (S. Xu).

https://doi.org/10.1016/j.jes.2024.01.002
1001-0742/

The highest detected residues of BPA have been reported 48 ng/g in peas (Noonan et al., 2011), 30 ng/g in green beans (Noonan et al., 2011), and 82 ng/g in corn (Yoshida et al., 2001). However, the greater concern lies in the residues found in canned foods. Epoxy resins and polyvinyl chloride organic solvents are commonly used as inner linings in cans to prevent direct contact between the metal surface and the food, thereby protecting the cans from corrosion (Cao et al., 2011). In Canada (Cao et al., 2010), the highest recorded BPA residue in canned food reached 534 ng/g, in the United States (Noonan et al., 2011) it was 730 ng/g, and in Japan, this alarming figure reached a staggering 842 ng/g (Sajiki et al., 2007). These data surpass the tolerable daily intake of BPA mentioned in the risk assessment published by the European Food Safety Authority, which is 50 μg/kg. BPA contamination has become an integral part of our daily lives that cannot be ignored. BPA exhibits neurotoxicity (Ha and Snyder, 1999), reproductive toxicity (Mir et al., 2020), hepatotoxicity (Chen et al., 2022b), and immunotoxicity (Qian et al., 2023). Furthermore, Qian et al. (2023) study reveals that BPA exposure can cause immune damage in zebrafish. The research conducted by Rochester et al. (2013) indicates that exposure to BPA can disrupt signal pathway transduction and stimulate the activity of inflammasomes in human bone marrow cells. Another study demonstrates that BPA induces NLRP3/caspase1/GSDMD pathway activation, leading to pyroptosis in human neuroblastoma cells. Additionally, Chen et al. (2023) reveals that BPA induces abnormal development of mouse fetal hearts by promoting ferroptosis.

Oxidative stress is a pathological process in which the redox balance is disrupted in cells following external stimuli, leading to cellular damage and death (Geethika et al., 2023). Extensive research has indicated that oxidative stress can induce apoptosis, necroptosis (Wang et al., 2022b), pyroptosis (Song et al., 2021), and ferroptosis (Han et al., 2022) in cells, causing tissue damage and impacting biological functions. Upon disruption of the intracellular redox balance, a significant accumulation of difficult-to-clear reactive oxygen species (ROS) occurs, leading to alterations in protein folding and triggering endoplasmic reticulum (ER) stress (Tripathi et al., 2022). Extensive research has demonstrated that an overload of ROS within cells can induce endoplasmic reticulum stress (Li et al., 2023; Wang et al., 2022a). Oxidative stress-mediated ER stress is closely associated with pyroptosis. The research conducted by Shi et al. demonstrates that particulate matter exposure regulates ER stress and NLRP3 inflammasome-mediated pyroptosis in mouse lungs through the Nrf2/HO-1/NQO1 pathway (Shi et al., 2023). Similarly, the crosstalk between ER stress and oxidative stress in the hippocampus of mice can lead to neuronal pyroptosis (Zhang et al., 2020). Moreover, research has demonstrated the regulatory role of oxidative stress-mediated ER stress in ferroptosis. Lan et al.'s research indicates that Saikosaponin A triggers ferroptosis in hepatocellular carcinoma cells through oxidative stress-mediated ER stress, stimulated by ATF3 expression (Lan et al., 2023). Additionally, Ma et al. demonstrate that silica induces macrophage ferroptosis by modulating oxidative stress/ER stress in mice. Similarly, Pu et al.'s study suggests that a high-potassium environment in cells can alleviate the occurrence of ferroptosis by inhibiting oxidative stress/ER stress (Pu et al., 2022).

As an essential trace element in biological processes, selenium plays an irreplaceable role in the organism through the circulatory system (Yang et al., 2022), digestive system (Xiao et al., 2021), urinary system (Chen et al., 2022a), and immune system (Liu et al., 2023b). Mice fed with a low-selenium diet exhibit a significant decrease in thymus index and an increase in inflammatory levels (Li et al., 2018). The study also indicates a reduction in G1/G2 phase cells and an increase in serum IL-2 levels in thymus tissue (Peng et al., 2011). Additionally, Chen et al. (2022a) reveals that selenium deficiency can induce autophagy in chicken kidneys induced by BPA. However, (1) Whether the exposure of BPA and Se deficiency can induce chicken thymus injury through oxidative stress and endoplasmic reticulum stress. (2) Whether BPA exposure and Se deficiency can induce thymus tissue injury by inducing pyroptosis and ferroptosis in the thymus lymphocyte. (3) Whether oxidative stress and ER stress mediate pyroptosis and ferroptosis in the thymus lymphocyte. (4) Whether the combined toxicity of BPA and selenium deficiency co-exposure is greater than that of single exposure was unclear. Therefore, our study aims to investigate the mechanisms of oxidative stress-mediated ER stress/pyroptosis and ferroptosis induced by combined exposure to BPA and selenium deficiency. To achieve this, we established Se deficiency or/and BPA exposure models in broiler chickens and MDCC-MSB-1 cells. We assess the content of peroxide MDA and H2O2, antioxidant enzymes T-AOC, SOD, and GSH-Px. We also measured the iron ion content in thymus tissues and MDCC-MSB-1 by iron assay kits and free orange staining. The membrane potential of mitochondria was explored using JC-1 staining. Immunofluorescence was used to evaluate the levels of pyroptosis in tissue and cellular. Furthermore, we detect the expression of ER stress-related genes (GRP78, IRE1, PERK, EIF-2α, ATF4, CHOP), ferroptosis-related genes (GPX4, TRC, HO-1, FTH, COX2, NADPH), and pyroptosis-related genes (NLRP3, ASC, Caspase1, GSDMD, IL-18, IL-1β) at both the mRNA and protein levels. This research aims to elucidate the mechanisms of damage in the broiler chicken thymus caused by BPA and selenium deficiency exposure and provides reliable evidence for immune damage caused by BPA and selenium deficiency.

1. Material and method

1.1. Main materials

BPA (Cas:80–05–7, purity≥99.0%) was purchased from Macklin reagent company; Na_2SeO_3 (Cas: GB8254–87, purity≥98%) was purchased from Chengdu Longquan Trace Elements Factory; RPMI-1640 (Cas: PM150110), Fetal bovine serum (VivaCell, Shanghai, China) was purchased from Priscilla Reagent Company; NAC (Sigma, A7250), TUDCA (35807-85-3) was purchased from sigma Reagent Company; Vx765 (S2228) was purchased from Selleckchem Reagent Company.

1.2. *Animal treatment*

The Northeast Agricultural University Ethics Committee (NEAUEC2023–03,111, China) gave its approval to all experimental methods. Sixty one-day-old chicks were randomly divided into four groups purchased from Harbin Xinghua breeder farm (15 chicks per group): Control group (BPA: 0 μg/kg; Selemiun (Se): 0.278 mg/kg), BPA group (BPA: 50 μg/kg; Se: 0.278 mg/kg), -Se group (BPA: 0 μg/kg; Se: 0.039 mg/kg), and BPA-Se group (BPA: 50 μg/kg; Se: 0.039 mg/kg). BPA and/or Se were uniformly mixed into the daily feed. The chicks were provided with free access to water and feed, and all other growth conditions were kept constant except for the diet. After 42 days, the chicks were euthanized, and fresh thymus tissues were collected and stored at −80 °C. Additionally, tissue blocks measuring 1 cm*1 cm*1 cm were fixed in 4% polyformaldehyde for subsequent experiments.

1.3. *HE staining*

Fixed thymus tissue embedded in a formaldehyde solution was trimmed to obtain a 1.0 cm * 1.0 cm * 0.3 cm thick tissue block. Dehydration was performed using various alcohol concentrations, followed by clearing in xylene, embedding in paraffin, and sectioning using a microtome to obtain 5 μm thin slices. The sections were stained with hematoxylin and eosin, and the slides were observed under an optical microscope.

1.4. *Transmission electron microscope (TEM)*

Fresh thymus tissue was cut into 0.3 cm * 0.3 cm * 0.3 cm cubes and placed in a 2.5% glutaraldehyde solution (Beyotime) at 4 °C overnight. After washing with phosphate buffer three times, the tissue was fixed with 1% osmium tetroxide for 2 hr. Dehydration was performed using different concentrations of alcohol, and the tissue was then sectioned into slices smaller than 80 nm using a microtome. The sections were mounted on copper grids and stained with uranyl acetate and lead citrate before observation and photography using a TEM (JEOL GEM-1200ES).

1.5. *Cell viability assessment and group culturing*

MDCC-MSB-1 cells were cultured in a CO_2 incubator maintained at 37 °C with 5% CO_2. The medium was changed every 24 hr, and passaging was performed every 48 hr. The Cell Counting Kit-8 (CCK-8) assay was used to measure the viability of MDCC-MSB-1 cells in response to BPA treatment. A total of 1.0×10^5 cells were seeded in each well of a 96-well plate and treated with culture medium containing different concentrations of BPA. After 24 hr, 10 μL of CCK-8 reagent was added to each well, and the plate was incubated at 37 °C for 30 min. The absorbance of each well was then measured at a wavelength of 450 nm using an Epoch microplate reader. BPA was diluted in dimethyl sulfoxide (DMSO) and stored at 4 °C (Wang et al., 2023b). The concentrations of BPA in the culture medium were 10, 20, 30, 50, 100, 200, 300, and 500 μmol/L, with a DMSO content of less than 0.1%. Based on the results, a concentration of 50 μmol/L was selected for the subsequent experiments.

The control group was cultured in a basal medium composed of 1640 supplemented with 1% fetal bovine serum (FBS), 10 μg/mL insulin, 5 μg/mL transferrin, and 50 ng/mL Na_2SeO_3. The BPA group was cultured in the basal medium supplemented with 50 μmol/L BPA. The low selenium group was cultured in a low selenium medium composed of 1640 supplemented with 1% FBS, 10 μg/mL insulin, and 5 μg/mL transferrin. The low selenium + BPA group was cultured in the low selenium medium supplemented with 50 μmol/L BPA. The low selenium + BPA + NAC group was cultured in the low selenium medium supplemented with 50 μmol/L BPA and 20 μmol/L NAC. The low selenium + BPA + Vx765 group was cultured in the low selenium medium supplemented with 50 μmol/L BPA and 30 μmol/L Vx765. The low selenium + BPA + TUDCA group was cultured in the low selenium medium supplemented with 50 μmol/L BPA and 300 μmol/L TUDCA.

1.6. *Immunofluorescence staining*

To assess the extent of pyroptosis in thymic tissue, we performed dual immunofluorescence staining on thymic tissue and MDCC-MSB-1 cells. The specific method was referenced from the article by Professor Xu et al. For primary antibodies, we used rabbit monoclonal antibodies against NLRP3 (1:200, Wanlei) and GSDMD (1:200, Bioss bs-14287R). For secondary antibodies, we used Dlight 594-conjugated anti-rabbit IgG (1:500) and Dlight 488-conjugated anti-rabbit IgG (1:500, Biodragon). DAPI staining (1:500, Beyotime, China) was used to label the cell nucleus. Fluorescent images were captured using a fluorescence microscope, and the fluorescence intensities of NLRP3 and GSDMD were analyzed using Image J (Lei et al., 2023).

1.7. *Detection of selenium content in thymus*

The selenium content in thymus tissue and feed was measured using inductively coupled plasma mass spectrometry (ICP-MS). 1 g thymus tissue was weighed and freeze-dried, then ground into a fine powder. The powdered samples were then mixed with 6 mL of nitric acid and subjected to microwave digestion. After cooling and acid evaporation to 1 mL, the solution was diluted to a final volume of 50 mL using deionized water. The selenium content in the prepared samples was quantitatively analyzed using an ICP-MS instrument (iCAPQ, Thermo, USA).

1.8. *Detection of BPA content in thymus*

Take 0.1 g of thymus tissue, grind and homogenize it, centrifuge at 3500 r/min for 10 min, and collect the supernatant. BPA assay kit for detecting the content of BPA in the thymus (Chenglin, Beijing).

1.9. *Detection of oxidative stress*

Take 0.1 g of fresh thymus tissue from each group of chicken breasts, add 1 mL of physiological saline for grinding. Each group of the above-mentioned grouped cells contains 10^6 cells. Perform sonication and centrifuge at 4 °C (4000 r/min,

15 min). Take the supernatant for the determination of oxidative stress-related enzyme activity. Use the Thermo Peroxidase (TP, A045–2–2, Nanjing Jiancheng, USA) method to detect the total protein concentration (Wang et al., 2023a). Calculate the activities of antioxidant enzymes such as GSH-PX (A005–1–2), T-AOC (A015–2–1), and CAT (A007–1–1). Measure the levels of MDA (A007–1–1) and H2O2 (A007–1–1) as indicators of lipid peroxidation and hydrogen peroxide content, respectively.

1.10. *Detection of tissue iron content and lactate dehydrogenase (LDH)*

After the aforementioned processing of the thymus tissue according to 2.9, collect the supernatant. Calculate the iron content in the thymus tissue (A039–2–1, Nanjing Jiancheng, China) and measure the activity of lactate dehydrogenase (LDH) (A020–1–2) based on the total protein concentration in the supernatant.

1.11. *Detection of ROS level*

After the aforementioned treatment for 24 hr, the oxidative stress levels of the cells in each group were assessed using a ROS assay kit (E11–004–1, NanjingJiancheng, China) (Li et al., 2024). The cells were placed under a fluorescence microscope, and three random fields of view were selected for photography. The obtained images were analyzed using Image J software to quantify the fluorescence intensity of the cells in each group.

1.12. *Detection of cellular mitochondrial function*

We used JC-1 as a fluorescent probe and utilized the ΔΨm Detection Kit (Beyotime Biotechnology) to measure the mitochondrial membrane potential of the cells in each group mentioned above. A decrease in mitochondrial membrane potential indicates mitochondrial dysfunction. After the aforementioned cell treatments, the cells were washed twice with PBS. Then, 250 nmol/L MitoTracker Green dye was added to each well and incubated for 30 min. The cells were observed under a fluorescence microscope, and three random fields of view were selected for photography. The acquired images were analyzed using Image J software to quantify the fluorescence intensity of the cells in each group.

1.13. *FerroOrange staining for the detection of cellular Fe^{2+} content*

After the aforementioned treatment for 24 hr, the cellular iron ion content in each group was measured using the FerroOrange detection kit (Tongren F374). The culture medium was removed, and the cells were washed three times with HBSS solution. Then, 1 μmol/L FerroOrange working solution was added to the cells and incubated at 37 °C in a 5% CO_2 incubator for 30 min. The cells were observed under a fluorescence microscope.

1.14. *RNA preparation and RT-PCR*

Extracting total RNA from 0.1 g of thymus tissue and reverse transcription of mRNA for cDNA Synthesis using reverse transcription kit. Amplification of cDNA using LineGene9600Plus Detection System, with Primer Design using Online Primer Design Software (Appendix A Table S1) and preparation of Master Mix with SYBR Green fluorescent dye (BSB25L1 B, BioFlux) (Zhang et al., 2022). β-actin is a stable housekeeping gene.

1.15. *Western blot*

Collect 0.1 g of thymus tissue from each group or harvest 10^6 cells from each group after 24 hr. Add 500 μL of protein lysis buffer (Beijing Solarbio Science & Technology Co.Ltd., China) and 5 μL of PMSF protease inhibitor mixture to extract total cellular proteins. The protein samples from each group were analyzed by sodium dodecyl sulfate-polyacrylamide gel electrophoresis (SDS-PAGE) (Li et al., 2023). To digest the cellulose membrane, they were incubated overnight with primary antibodies (Appendix A Table S2), followed by washing with TBST and incubation with anti-rabbit IgG secondary antibody at room temperature in the dark for 2 hr. After washing three times with TBST, the gels were scanned using a gel imaging system, and the grayscale values of each protein band were analyzed using Image J software.

1.16. *Date analysis*

All experiments were performed in triplicate, and the data obtained were statistically analyzed using GraphPad Prism 9.3.0. One-way analysis of variance (ANOVA) was used to analyze the data from all groups on multiple dates, and the results were presented as mean ± standard deviation (mean ± SD). Independent samples were compared between the two groups. Different letters represent significant diversity between different groups, with statistical significance ($p < 0.05$) (Lv et al., 2023).

2. Results

2.1. *Establish models of BPA and/or low selenium* in vitro/vivo

As shown in Fig. 1A, we observed the morphology of thymus tissue through HE staining. The control group showed clear corticomedullary demarcation and well-defined medullary trabeculae. However, the BPA group displayed disrupted medullary structure with cell exfoliation (indicated by black arrows). The -Se group exhibited congestion at the corticomedullary junction with red blood cell infiltration (indicated by arrows). In the BPA-Se group, there was no intact cortical structure, and the medullary architecture was disordered (highlighted by black arrows). These findings indicate that BPA exacerbates thymic injury induced by -Se.

To verify the success of the model establishment, we tested the levels of BPA and Se in the chicken thymus as shown in Fig. 1B. In the BPA group, the BPA content in the thymus was 1.74 μg/L, significantly higher than the Control group and -Se group ($p < 0.05$). However, in the BPA-Se group, the BPA content in the thymus was 3.24 μg/L, significantly higher than the BPA group ($p < 0.05$). In Fig. 1C, the -Se group had a selenium content of 0.080 mg/kg, significantly lower than the Control

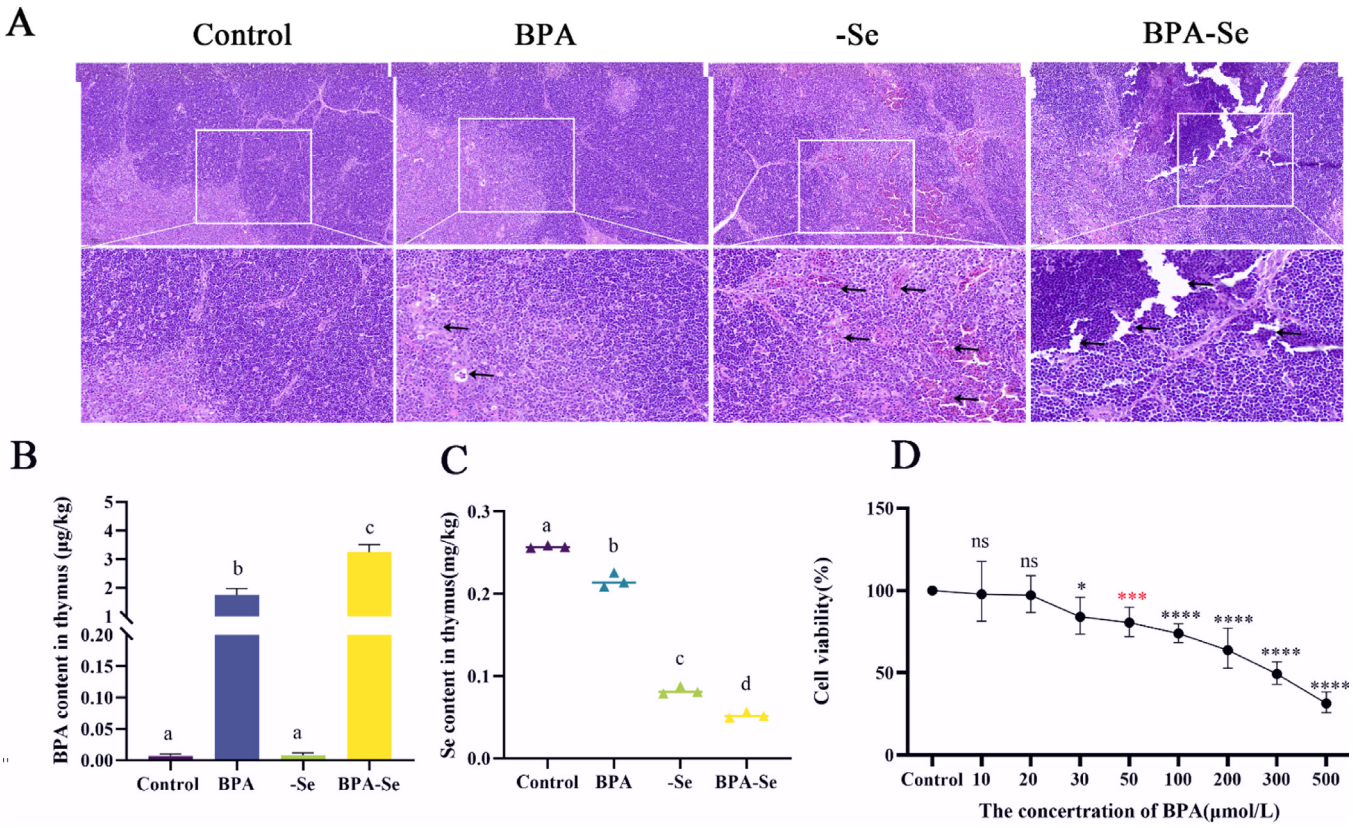

Fig. 1 – Results of HE staining, selenium content and BPA levels in thymus, and the effect of BPA on MDCC-MSB-1 cell viability. (A) The results of the HE staining showed varying degrees of thymic tissue damage in different groups. The black arrows indicate the extent of thymic injury observed in the samples Scale bar: 50 μm and 100 μm. (B) BPA content (μg/L) in chicken thymus of each group ($n = 3$). (C) Se content (mg/kg) in chicken thymus of each group ($n = 3$). (D) Viability of MDCC-MSB-1 cells treated with different concentrations of BPA (10 μmol/L 20 μmol/L, 30 μmol/L, 50 μmol/L, 100 μmol/L, 200 μmol/L, 300 μmol/L, 500 μmol/L) ($n = 3$). Note: The same letter represents no significant difference between groups ($p > 0.05$), while different letters represent significant differences between groups ($p < 0.05$), ns: Represent there was no significant differences compared to the control group ($p > 0.05$), *: Represent significant differences compared to the control group ($p < 0.05$), *: The BPA concentration was chosen for subsequent experiments and has significant differences compared to the control group ($p < 0.01$), ****: Represent significant differences compared to the control group ($p < 0.001$). MDCC-MSB-1: Chicken lymphoma cells.**

group ($p < 0.05$). Interestingly, in the BPA-Se group, the thymus selenium content was 0.051 mg/kg, significantly lower than the -Se group ($p < 0.05$). These results indicate that low selenium exacerbates the accumulation of BPA in the thymus, and simultaneously, BPA interferes with the uptake of trace elements in the thymus.

In vitro model establishment, the CCK8 assay was used to assess the toxicity of BPA on MDCC-MSB-1 cells. According to Prism calculations, the IC50 of BPA is 285.1 μmol/L (with a 95% confidence interval of 238.6 μmol/L to 350.2 μmol/L). As shown in Fig. 1D, at a BPA concentration of 50 μmol/L, the cell viability was measured to be 80.87%. This concentration was used for the next step of the experiment.

2.2. *BPA exacerbates selenium deficiency-induced oxidative stress in chicken thymus*

Oxidative stress results from an imbalance in the redox system caused by an increase in intracellular ROS and a decrease in antioxidant enzyme activity, leading to the promotion of disease occurrence and development. Firstly, we measured the levels of ROS through the activities of antioxidant enzymes and the peroxide in the chicken thymus homogenate. The results demonstrated that in Fig. 2A, compared to the control group, both the BPA and Se groups exhibited significantly reduced activities of antioxidant enzymes (T-AOC, CAT, and GSH-Px) and significantly increased levels of ROS (MDA and H_2O_2) ($p < 0.05$). Meanwhile, the co-treated group showed significantly more pronounced changes compared to the individually exposed group ($p < 0.05$). Similar results were observed in the in vitro model (Fig. 2B).

Additionally, the DCFH-DA staining of MDCC-MSB-1 cells, as shown in Fig. 2C-D, revealed that the intracellular fluorescence intensity increased significantly in both the BPA and -Se individually exposed groups when compared to the Control group. Furthermore, the co-exposure group exhibited a more significant increase in intracellular fluorescence intensity compared to the individually exposed groups. Moreover,

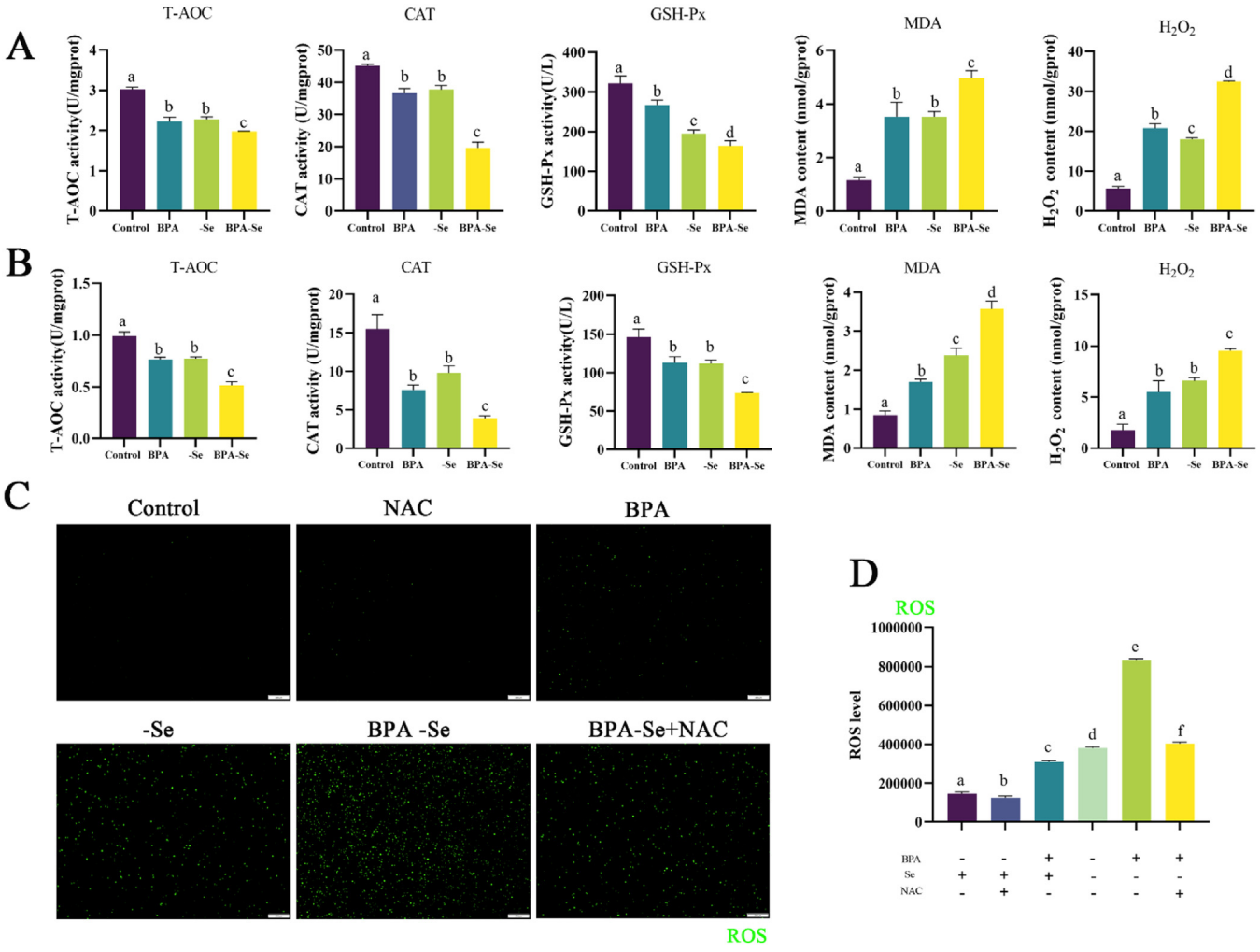

Fig. 2 – Determination of antioxidant enzymes viability and peroxides content in chicken thymus tissues and MDCC-MSB-1, and determination of ROS level in MDCC-MSB-1: (A) Quantitative analysis of antioxidant enzymes (T-AOC, CAT, GSH-Px) and peroxides (MDA, H_2O_2) in homogenates of chicken thymus tissues ($n = 3$). (B) Measurement of antioxidant enzymes (T-AOC, CAT, GSH-Px) and peroxides (MDA, H_2O_2) in MDCC-MSB-1 cells ($n = 3$). (C) Fluorescence images of intracellular reactive oxygen species (ROS) detected using DCFH-DA probe in different groups (Control, NAC, BPA, -Se, BPA-Se, BPA-Se+NAC) of MDCC-MSB-1. (D) Quantification of fluorescence intensity in each group of cells ($n = 3$). Note: The same letter represents no significant difference between groups ($p > 0.05$), while different letters represent significant differences between groups ($p < 0.05$). MDCC-MSB-1: Chicken lymphoma cells; T-AOC: Total antioxidant capacity; CAT: Catalase; GSH-Px: Glutathione peroxidase; MDA: Malonic dialdehyde; H_2O_2: Hydrogen peroxide; ROS: Reactive oxygen species.

the addition of N-acetylcysteine (NAC) significantly reduced the fluorescence levels in the BPA-Se co-exposure group, Therefore, for the subsequent experiments, NAC was used as an antioxidant.

2.3. *BPA exacerbates ER stress and apoptosis induced by selenium deficiency in chicken thymus tissue*

Aberrant overexpression of NLRP3 and GSDMD proteins serves as markers for pyroptosis, thus we examined the expression levels of these two proteins from different perspectives. Compared to the Control group, the fluorescence intensity of NLRP3 (in red) and GSDMD (in green) significantly increased in the BPA or -Se individually exposed groups (Fig. 3A-B) ($p < 0.05$). Furthermore, the fluorescence intensity in the co-exposure group showed a significant increase compared to the individually exposed groups ($p < 0.05$). The activity of lactate dehydrogenase (LDH), a soluble marker of pyroptosis, was assessed in the homogenate of chicken thymus tissues using an LDH assay kit. The results (Fig. 3C) revealed that, compared to the Control group, the LDH activity increased significantly in the individually exposed groups ($p < 0.05$). Additionally, in the co-exposure group, LDH activity showed a significant increase compared to the individually exposed groups ($p < 0.05$). From both mRNA (Fig. 3G) and protein (Fig. 3E) perspectives, the expression of pyroptosis-related genes (NLRP3, ASC, Caspase-1,

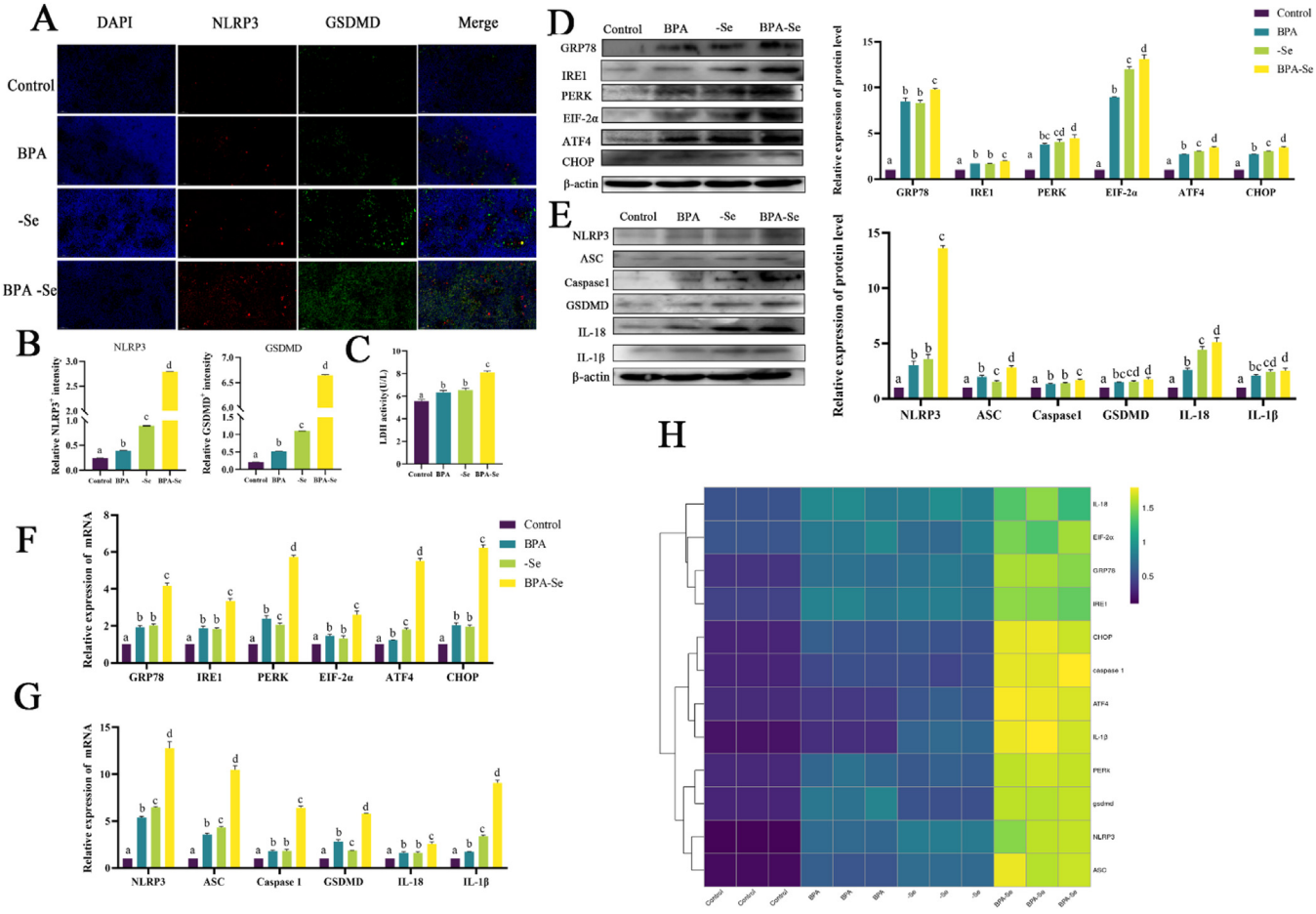

Fig. 3 – Effects of BPA and Se deficiency on ER Stress and pyroptosis in thymus tissues: (A) Immunofluorescence images of NLRP3 (Red) and GSDMD (Green) in thymus tissues, DAPI (Blue) was nucleus. Scale bar: 50 μm. (B) Quantification of total fluorescence intensity of NLRP3 and GSDMD in thymus tissues ($n = 3$). (C) The activity of LDH in the tissue homogenization ($n = 3$). (D) Protein expression levels and quantification of ER stress-related genes (GRP78, IRE1, PERK, EIF-2α, ATF-4, CHOP) in thymus tissues ($n = 3$). (E) Protein expression levels and quantification of pyroptosis-related genes (NLRP3, ASC, Caspase 1, GSDMD, IL-18, IL-1β) in thymus tissues ($n = 3$). (F) Gene expression levels of ER stress related genes (GRP78, IRE1, PERK, EIF-2α, ATF-4, CHOP) in thymus tissues ($n = 3$). (G) Gene expression levels of pyroptosis-related genes (NLRP3, ASC, Caspase 1, GSDMD, IL-18, IL-1β) in thymus tissues ($n = 3$). (H) Heatmap results of related genes (GRP78, IRE1, PERK, EIF-2α, ATF-4, CHOP, NLRP3, ASC, Caspase 1, GSDMD, IL-18, IL-1β) in thymus tissues. The data has been log2 transformed and the expression of mRNA represent increase from blue to yellow ($n = 3$). Note: The same letter represents no significant difference between groups ($p > 0.05$), while different letters represent significant differences between groups ($p < 0.05$). MDCC-MSB-1: Chicken lymphoma cells, LDH: Lactate dehydrogenase.

GSDMD, IL-18, and IL-1β) significantly increased in the BPA or groups ($p < 0.05$). Furthermore, in the co-exposure group, the expression of these genes showed a significant increase compared to the individually exposed groups ($p < 0.05$).

ER stress refers to the inhibition of protein folding within the cell, leading to protein accumulation or abnormal folding, which is widely present in cellular pathological conditions. As shown in the figures, compared to the Control group, the expression of ER-related genes (GRP78, IER1, PERK, EIF-2α, ATF4, and CHOP) significantly increased in the BPA or -Se groups in the mRNA (Fig. 3F) and protein (Fig. 3D) levels ($p < 0.05$). Furthermore, in the co-exposure group, the expression of these genes showed a significant increase compared to the individually exposed groups ($p < 0.05$).

2.4. *BPA aggravates selenium deficiency-induced pyroptosis in MDCC-MSB-1 cells through ROS/ER stress*

To investigate the relationship among oxidative stress, ER stress, and pyroptosis, we employed MDCC-MSB-1 cells as the experimental model. Immunofluorescence results (Fig. 4A-B) revealed that compared to the Control group, the fluorescence intensity of NLRP3 and GSDMD significantly increased in the groups exposed to BPA or -Se alone ($p < 0.05$). Moreover, the co-exposure group exhibited a significant increase in fluorescence intensity compared to the single-exposure groups ($p < 0.05$). Compared to the Control group, the groups exposed to BPA or -Se alone showed significant upregulation of ER stress-related genes (GRP78, IER1, PERK, EIF-2α, ATF4, and CHOP and

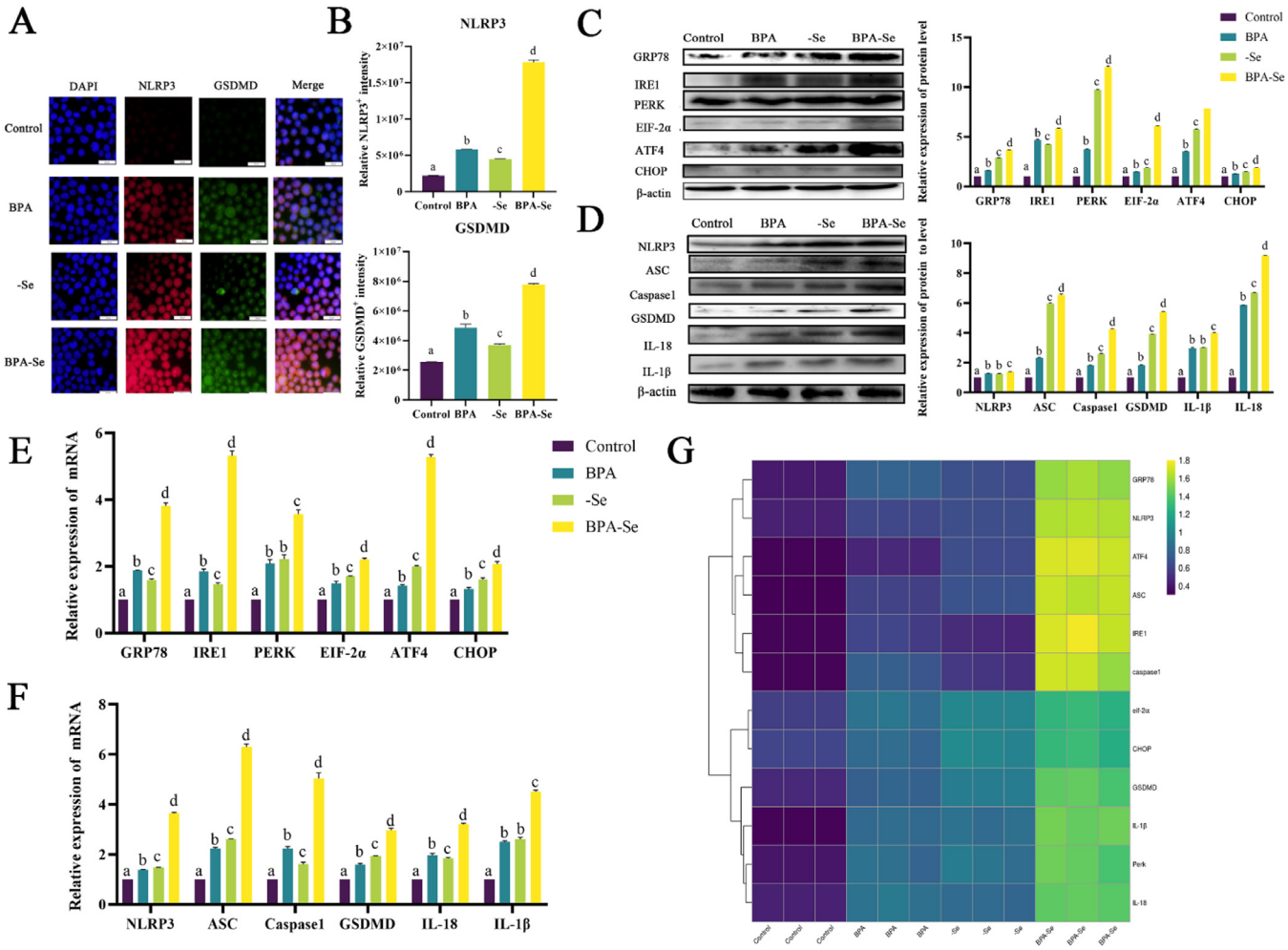

Fig. 4 – Effects of BPA and Se deficiency exposure on ER Stress and pyroptosis related gene expression in MDCC-MSB-1 cells: (A) Immunofluorescence staining of NLRP3 (Red) and GSDMD (Green) in MDCC-MSB-1 cells. DAPI (Blue) was nucleus. Scale bar: 20 μm. (B) Quantification of total fluorescence intensity of NLRP3 (Red) and GSDMD (Green) in MDCC-MSB-1 cells ($n = 3$). (C) Protein expression levels and quantification of ER stress-related genes (GRP78, IRE1, PERK, EIF-2α, ATF-4, CHOP) in MDCC-MSB-1 cells ($n = 3$). (D) Protein expression levels and quantification of pyroptosis-related genes (NLRP3, ASC, Caspase1, GSDMD, IL-18, IL-1β) in MDCC-MSB-1 cells ($n = 3$). (E) Gene expression levels of ER stress-related genes (GRP78, IRE1, PERK, EIF-2α, ATF-4, CHOP) in MDCC-MSB-1 cells. (F) Gene expression levels of ER stress-related genes (NLRP3, ASC, Caspase1, GSDMD, IL-18, IL-1β) in MDCC-MSB-1 cells. (G) Heatmap results of related genes (GRP78, IRE1, PERK, EIF-2α, ATF-4, CHOP, NLRP3, ASC, Caspase1, GSDMD, IL-18, IL-1β) in MDCC-MSB-1 cells. The data has been log2 transformed and the expression of mRNA represent increase from blue to yellow ($n = 3$). Note: The same letter represents no significant difference between groups ($p > 0.05$), while different letters represent significant differences between groups ($p < 0.05$), MDCC-MSB-1: Chicken lymphoma cells.

pyroptosis-related genes (NLRP3, ASC, Caspase1, GSDMD, IL-18, and IL-1β) at both mRNA and protein levels ($p < 0.05$). Additionally, compared to the single-exposure groups, the co-exposure group exhibited a significant elevation of the related genes at both mRNA (Fig. 4E-H) and protein levels (Fig. 4C-D) ($p < 0.05$).

To investigate the crosstalk between oxidative stress, ER stress, and apoptosis. For this purpose, we established three treatment groups: the BPA-Se+TUDCA group, BPA-Se+Vx765 group, and BPA-Se+NAC group. Detect the expression of ER stress-related genes and pyroptosis-related genes at different levels in each group. Treatment with the ER stress inhibitor (TUDCA) and the pyroptosis inhibitor (Vx765) remarkably reduced the fluorescence intensity induced by joint exposure to BPA and Se deficiency ($p < 0.05$). Meanwhile, the results revealed that both NAC and TUDCA treatments significantly alleviated the upregulation of ER stress and pyroptosis-related genes induced by combined exposure in mRNA (Fig. 5C-G) and protein levels (Fig. 5H-K) ($p < 0.05$). Vx765 treatment. On the other hand, effectively mitigated the upregulation of pyroptosis-related genes ($p < 0.05$) induced by combined exposure but did not alleviate changes in ER stress-related genes in the mRNA (Fig. 5C-E) and protein levels (Fig. 5H-I) ($p < 0.05$). These findings indicate that BPA in conjunction with

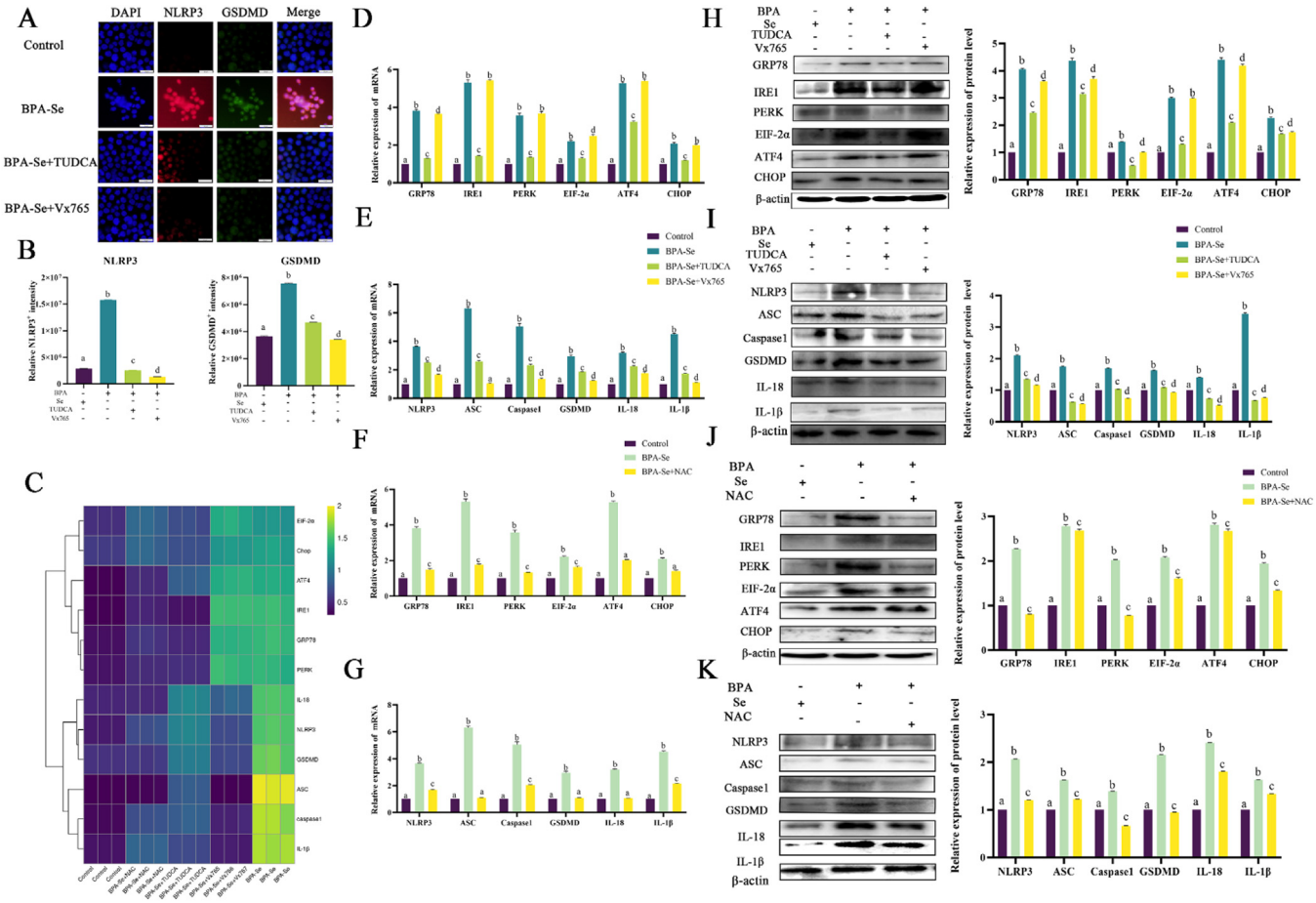

Fig. 5 – BPA and Se deficiency exposure induce pyroptosis in MDCC-MSB-1 cells through oxidative stress/ER stress: (A) Immunofluorescence staining of NLRP3 (Red) and GSDMD (Green) in MDCC-MSB-1 cells. DAPI (Blue) was nucleus. Scale bar: 20 μm. (B) Quantification of total fluorescence intensity of NLRP3 and GSDMD in MDCC-MSB-1 cells ($n = 3$). (C) Heatmap results of related genes (GRP78, IRE1, PERK, EIF-2α, ATF-4, CHOP, NLRP3, ASC, Caspase 1, GSDMD, IL-18, IL-1β) in MDCC-MSB-1 cells. (D-G) The mRNA levels of ER stress-related (GRP78, IRE1, PERK, EIF-2α, ATF-4, CHOP) and pyroptosis-related genes (NLRP3, ASC, Caspase 1, GSDMD, IL-18, IL-1β) in the Control, BPA-Se, BPA-Se+TUDCA, BPA-Se+Vx765, and BPA-Se+NAC groups in MDCC-MSB-1 cells ($n = 3$). (H-K) The protein levels of ER stress-related (GRP78, IRE1, PERK, EIF-2α, ATF-4, CHOP) and pyroptosis-related genes (NLRP3, ASC, Caspase1, GSDMD, IL-18, IL-1β) in the Control, BPA-Se, BPA-Se+TUDCA, BPA-Se+Vx765, and BPA-Se+NAC groups in MDCC-MSB-1 cells ($n = 3$). Note: The same letter represents no significant difference between groups ($p > 0.05$), while different letters represent significant differences between groups ($p < 0.05$). MDCC-MSB-1: Chicken lymphoma cells. TUDCA: ER stress inhibitor. Vx765: Pyroptosis inhibitor. NAC: Oxidative stress inhibitor.

Se induces pyroptosis in MDCC-MSB-1 cells through oxidative stress/ER stress pathway (Fig. 5C).

2.5. *BPA aggravates low selenium to induce thymocyte ferroptosis through oxidative stress and ER stress*

Ferroptosis, characterized by cellular iron overload and mitochondrial dysfunction, is widely observed in various immunodeficiency diseases and mitochondrial shrinkage is a morphological feature of ferroptosis (Han et al., 2022). Observation of chicken thymus damage through transmission electron microscopy (TEM) as shown in Fig. 6A: In the Control group, the thymus tissue exhibited intact structural organization, normal mitochondrial morphology, and well-defined mitochondrial membranes and cristae. In the BPA group, mitochondrial morphology appeared normal; however, there were some vacuoles observed in the intercristal spaces, although the changes were not significantly different from the Control group. In the -Se group, mitochondrial morphology was abnormal, with widespread vacuolization and extensive cristae wrinkling. In the BPA-Se group, mitochondria exhibited circular shrinkage (as indicated by the arrows in the figure), significant cristae alterations, and vacuolization. These results collectively suggest that both BPA exposure and selenium deficiency induce damage to the chicken thymus. Meanwhile, the Fe^{2+} content results showed that BPA and Se significantly up-

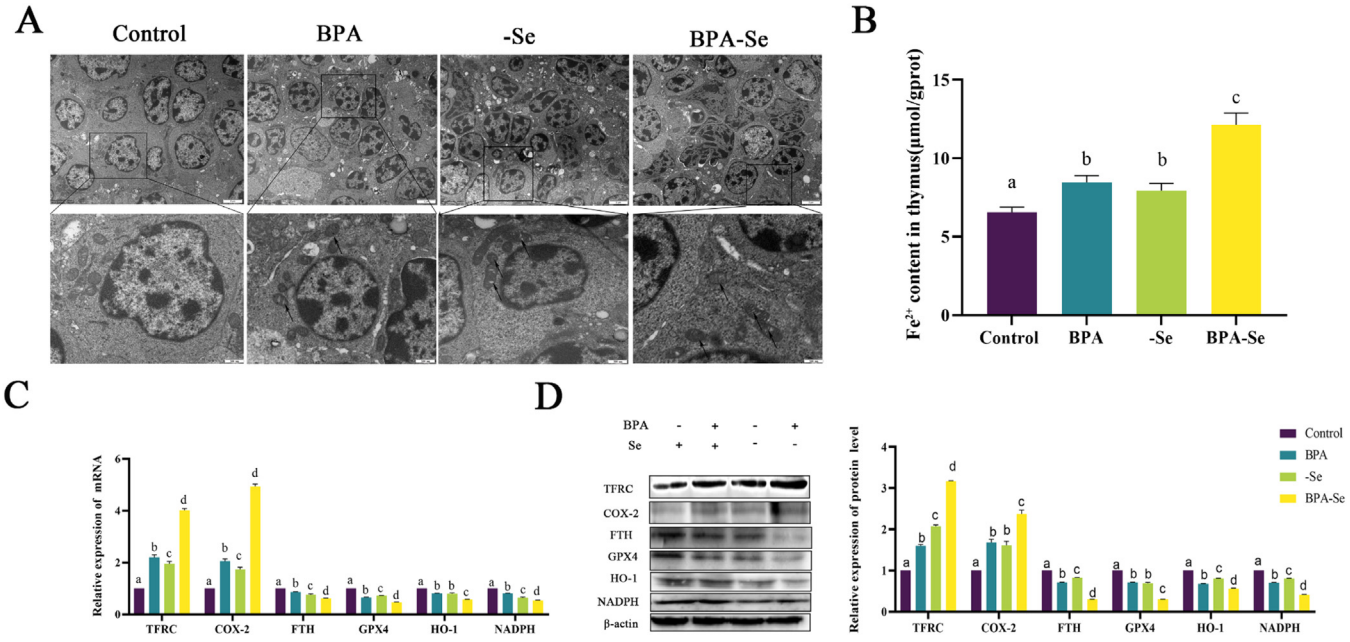

Fig. 6 – BPA and Se deficiency exposure induce ferroptosis in chicken thymic: (A) Transmission electron microscopy results of the Control group, BPA group, -Se group, and BPA-Se group. Scale bar: 2 μm. The black arrow points to mitochondrial morphological abnormalities. (B) Fe^{2+} content (μmol/gprot) in the chicken thymus of each group ($n = 3$). (C) Gene expression levels and quantification of ferroptosis-related genes (TFRC, COX-2, FTH, GPX4, HO-1, NADPH) ($n = 3$). (D) Protein expression levels and quantification of ferroptosis-related genes (TFRC, COX-2, FTH, GPX4, HO-1, NADPH). Note: The same letter represents no significant difference between groups ($p > 0.05$), while different letters represent significant differences between groups ($p < 0.05$). MDCC-MSB-1: Chicken lymphoma cells.

regulated ($p < 0.05$) the Fe^{2+} content in the tissues compared to the single exposures, and co-exposure further increased ($p < 0.05$) the Fe^{2+} content (Fig. 6B).

Furthermore, we examined the expression of ferroptosis-related genes. In vivo, compared to the Control group, exposure to BPA or Se deficiency led to a significant increase in the mRNA and protein levels of TFRC and COX-2, while mRNA (Fig. 6C) and protein (Fig. 6D) levels of FTH, HO-1, GPX4, and NADPH showed significant reductions($p < 0.05$).

On the other hand, similar results were obtained in vitro. We examined the mitochondrial membrane potential and iron ion content in cells from different groups. The results (Fig. 7A-B) showed a significant increase in green fluorescence and a decrease in red fluorescence in the BPA and -Se groups compared to the Control group ($p < 0.05$). The combined treatment group exhibited further enhancement of fluorescence intensity ($p < 0.05$). FerroOrange staining results indicated a significant increase in red fluorescence in the BPA and -Se groups compared to the Control group ($p < 0.05$), and the combined exposure group showed even higher ($p < 0.05$) red fluorescence compared to the individually exposed groups (Fig. 7C-D) Additionally, the expression of ferroptosis-related genes at both mRNA (Fig. 7G) and protein (Fig. 7E) levels in MDCC-MSB-1 cells yielded consistent results with those observed in vivo. Interestingly, to explore the crosstalk among oxidative stress, ER stress, and ferroptosis, we established BPA-Se+TUDCA and BPA-Se+NAC treatment groups. The results demonstrated that NAC and TUDCA treatments significantly alleviated the alterations in ER stress-related and ferroptosis-related genes both in mRNA (Fig. 7H) and protein (Fig. 7F) levels induced by combined exposure ($p < 0.05$). These findings indicate that BPA combined with low-Se induces ferroptosis in MDCC-MSB-1 cells through oxidative stress and ER stress pathway (Fig. 7I).

3. Discussion

The thymus is an essential central immune organ in organisms, and research has revealed that it is one of the target organs for the toxic effects of BPA (Dagher et al., 2021). BPA has been found to induce cellular autophagy (Park et al., 2023) and apoptosis (Sabry et al., 2023), as well as decrease cytokine secretion in cells. Selenium deficiency can lead to pathological changes in the immune organs of chickens, accompanied by reduced levels of IL-1β, IL-2, and TNF in serum (Zhang et al., 2012), as well as impaired immune function (Qiu et al., 2022). This study investigated the detrimental effects of BPA and/or selenium deficiency on the thymus of broiler chickens. The results revealed that exposure to BPA or selenium deficiency led to a significant increase in the levels of MDA and H_2O_2. There was also a significant decrease in antioxidant enzyme activity (T-AOC, SOD, and GSH-Px), while LDH activity in serum significantly increased. Furthermore, there was a significant increase in free iron ion levels, accompanied by thymic mitochondrial shrinkage and a decrease in mitochondrial membrane potential. The expression of ER stress-related genes (GRP78, IRE1, Perk, EIF-2α, ATF4, CHOP),

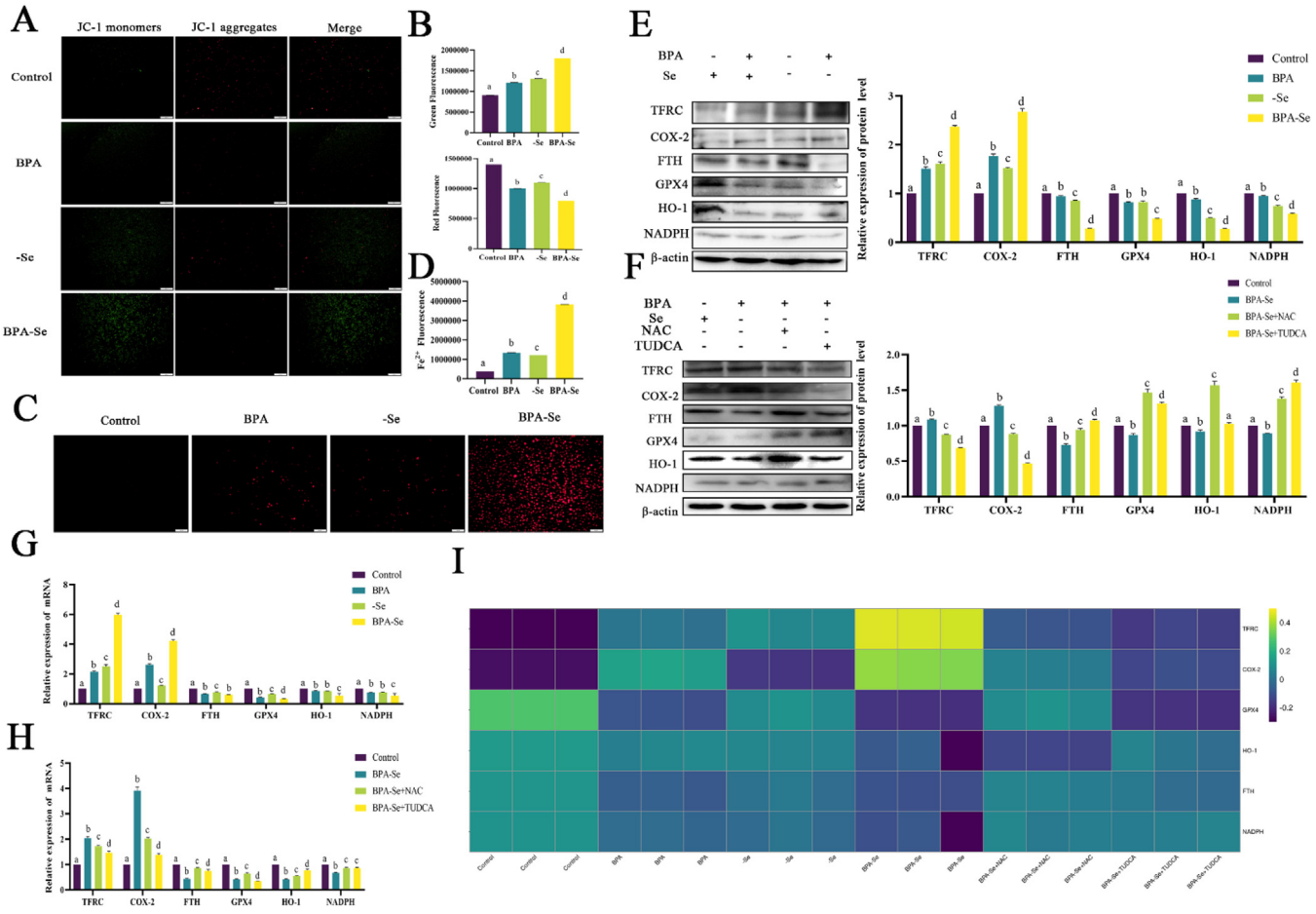

Fig. 7 – BPA and Se deficiency exposure induce ferroptosis in MDCC-MSB-1 Cells through oxidative stress/ER stress: (A-B) JC-1 staining to detect mitochondrial membrane potential in cells of each group, with corresponding quantification. Scale bar: 100 μm. Note: Green for JC-1 monomers and Red for JC-1 aggregates. (C-D) **FerroOrange staining to detect fluorescence in cells of each group with the corresponding quantification. Scale bar: 50 μm** (E-F) **The protein expression levels and quantification of ferroptosis-related genes (TFRC, COX-2, FTH, GPX4, HO-1, NADPH) in different groups (Control, BPA, -Se BPA-Se, BPA-Se+TUDCA, and BPA-Se+NAC) of MDCC-MSB-1 cells.** (G-H) **The Gene expression levels and quantification of ferroptosis-related genes in MDCC-MSB-1 cells.** (I) **Heatmap results of ferroptosis-related genes in MDCC-MSB-1 cells. Note: The same letter represents no significant difference between groups ($p > 0.05$), while different letters represent significant differences between groups ($p < 0.05$). MDCC-MSB-1: Chicken lymphoma cells. TUDCA: ER stress inhibitor. Vx765: Pyroptosis inhibitor. NAC: Oxidative stress inhibitor.**

pyroptosis-related genes (NLRP3, ASC, Caspase1, GSDMD, IL-18, IL-1β), and ferroptosis-related genes (TFRC, COX-2) showed a significant upregulation, whereas the expression of GPX4, HO-1, COX-2, and NADPH was downregulated. Moreover, the combined exposure group exhibited more pronounced effects on the aforementioned changes compared to the individual treatment groups.

Oxidative stress refers to the imbalance in the body's redox system, where an excess of ROS in tissues or cells leads to pathological damage. It is characterized by an overload of peroxides and a decline in antioxidant enzyme activity. Zhang et al. demonstrated that Pb-exposure induces an excessive generation of ROS in porcine testicular interstitial cells (Zhang et al., 2023). Additionally, the study by Chen et al. (2023) revealed that exposure to di(2-ethylhexyl) phthalate and microplastics led to the accumulation of peroxides (MDA, H_2O_2) in mouse liver cells, along with a significant decrease in antioxidant enzyme activity (T-AOC, MDA, and GSH). Furthermore, in poultry farming, Wang et al. found that lipopolysaccharide (LPS) exposure led to oxidative stress and the overproduction of oxygen-free radicals in chicken lungs (Wang et al., 2021). In our study, we also observed oxidative stress characterized by a significant increase in the levels of peroxides (MDA, H_2O_2), a significant decrease in antioxidant enzyme activity (T-AOC, SOD, GSH-Px), and a significant increase in intracellular ROS levels in the thymus and MDCC-MSB-1 cells under BPA exposure and selenium deficiency. Numerous studies have shown that oxidative stress can induce ER stress (Li et al., 2023; Liu et al., 2022; Xia et al., 2023). Evidence from gill tissue of carp, chicken heart, and human ischemia-reperfusion injury models has demonstrated that oxidative stress leads to ER stress, manifested by a significant upregulation of genes

such as GRP78, IRE1, and EIF2α. Similarly, our study found that BPA or selenium deficiency exposure led to a significant increase in the transcription and protein levels of ER stress-related genes (GRP78, IRE1, Perk, EIF-2α, ATF4, CHOP) in broiler chicken thymus tissue. Furthermore, compared to the individual treatment groups, the combined exposure group exhibited further elevation of the gene levels. Consistent results were obtained from in vitro experiments, where the addition of NAC significantly alleviated the changes in these genes, suggesting that oxidative stress regulates ER stress. This viewpoint is supported by Zhu et al. (2023). Taken together, these findings suggest that both BPA and selenium deficiency exposure can induce ER stress in broiler chicken thymus tissue through oxidative stress.

Ferroptosis is a novel form of cell death characterized by abnormal iron metabolism leading to intracellular accumulation of ROS and iron-dependent non-apoptotic cell demise (Guo et al., 2023). Extensive studies have indicated (Adham et al., 2020; Ba et al., 2022; Zhou et al., 2022) that thymic tissue undergoing iron death exhibits intracellular iron overload, increased peroxide levels, and significant alterations in iron death-related genes such as FTH. Our findings also revealed mitochondrial atrophy, a significant rise in Fe^{2+} levels, decreased mitochondrial membrane potential, Fe^{2+} accumulation, and a synergistic enhancement of these changes in tissues exposed to BPA or low selenium. Moreover, transferrin levels were significantly upregulated at the transcriptional and protein levels, triggering COX-2-mediated inflammation, while the expression of GPX4, HO-1, FTH, and NADPH were significantly decreased. Co-exposure to the aforementioned factors further intensified these alterations. Silica exposure was shown to induce iron death in mouse macrophages through ROS/ER stress (Ma et al., 2023). In a rat cardiac arrest model, oxidative stress/ER stress led to myocardial iron death (Ye et al., 2023). Similarly, our study demonstrated that BPA or low selenium exposure induced oxidative stress/ER stress and iron death in chicken thymic tissue and cells. Interestingly, the addition of NAC or TUDCA significantly alleviated the changes in ferroptosis-related genes in vitro. These results suggest that BPA combined with low selenium induces ferroptosis in chicken thymus through oxidative stress/ER stress.

The oxidative stress/ER stress pathway is involved in the regulation of pyroptosis. Many toxins can induce pyroptosis in multiple organs. For example, LPS exposure induces pyroptosis in pig spleen and thymus (Liu et al., 2023a), while aflatoxin exposure leads to pyroptosis and autophagy in pig thymus (Mocchegiani et al., 1998). Similarly, our study found that BPA or low selenium exposure caused a significant upregulation of pyroptosis-related genes (NLRP3, ASC, Caspase1, GSDMD, IL-18, IL-1β) at the mRNA and protein levels in chicken thymic tissue and cells. Additionally, LDH activity significantly increases in the tissue, and these changes are more pronounced in co-exposed conditions. Research has demonstrated that isoproterenol exposure induces cardiac myocyte pyroptosis in rats through oxidative stress/ER stress. Leptin induces pyroptosis in lung cancer cells through oxidative stress/ER stress (Baral and Park, 2021). The aforementioned experiments have shown that BPA and/or selenium deficiency induce ER stress through oxidative stress. Subsequent in vitro experiments with the addition of NAC or TUDCA were conducted to investigate the effects of ROS and ER stress on pyroptosis. It was found that ROS/ER stress is involved in the regulation of pyroptosis induced by BPA and/or selenium deficiency. Interestingly, the addition of Vx-765 significantly alleviates pyroptosis but does not alleviate ER stress, indicating that the influence of the ER on pyroptosis is unidirectional. These results suggest that BPA combined with low selenium induces pyroptosis in chicken thymus through oxidative stress/ER stress.

In summary, BPA combined with low selenium induces oxidative stress/ER stress in chicken thymic tissue, leading to pyroptosis and ferroptosis. In vitro experiments further demonstrated that the addition of NAC and TUDCA significantly alleviated pyroptosis and ferroptosis by inhibiting oxidative stress and ER stress, respectively.

4. Conclusion

In conclusion, BPA combined with low selenium activates pyroptosis and ferroptosis through oxidative stress/ER stress. This study elucidates the toxic mechanisms of BPA and low selenium on chicken thymus and provides insights for research on the toxicity of environmental pollutants and deficiency of trace elements.

Declaration of competing interest

The authors declare that they have no known competing financial interests or personal relationships that could have appeared to influence the work reported in this paper.

Acknowledgment

This work was supported by the National Natural Science Foundation of China Regional Joint Innovation Fund (No. U22A20524) and the Heilongjiang Province Natural Science Foundation Key projects (No. ZD2023C002).

Appendix A Supplementary data

Supplementary material associated with this article can be found, in the online version, at doi:10.1016/j.jes.2024.01.002.

References

Adham, A.N., Hegazy, M.E.F., Naqishbandi, A.M., Efferth, T, 2020. Induction of apoptosis, autophagy and ferroptosis by thymus vulgaris and arctium lappa extract in leukemia and multiple myeloma cell lines. Molecules 25. https://pmc/articles/PMC7663330/.

Ba, T., Zhao, D., Chen, Y., Zeng, C., Zhang, C., Niu, S, 2022. L-citrulline supplementation restrains Ferritinophagy-mediated ferroptosis to alleviate iron overload-induced thymus oxidative damage and immune dysfunction. Nutrients. 14. https://pmc/articles/PMC9655478/.

Baral, A., Park, P.H., 2021. Leptin induces apoptotic and pyroptotic cell death via NLRP3 inflammasome activation in rat

hepatocytes. Int. J. Mol. Sci. 22. https://pmc/articles/PMC8622994/.
Cao, X.L., Corriveau, J., Popovic, S., 2010. Bisphenol A in canned food products from Canadian markets. J. Food Prot. 73, 1085–1089. doi:10.4315/0362-028X-73.6.1085.
Cao, X.L., Perez-Locas, C., Dufresne, G., Clement, G., Popovic, S., Beraldin, F, 2011. Concentrations of bisphenol A in the composite food samples from the 2008 canadian total diet study in quebec city and dietary intake estimates. Food Addit. Contam. Part A Chem. Anal. Control Expo. Risk Assess. 28, 791–798. https://pmc/articles/PMC3118530/.
Chen, Y.J., Zhang, M., Li, S.S., Wang, W., Wang, Y.P., Yi, C.H., 2023. Exposure To bisphenol A induces abnormal fetal heart development by promoting ferroptosis. Ecotoxicol. Environ. Saf. 255, 114753. doi:10.1016/j.ecoenv.2023.114753.
Chen, H., Zhang, Y., Qi, X., Shi, X., Huang, X., Xu, S.W., et al., 2022a. Selenium deficiency aggravates bisphenol A-induced autophagy in chicken kidney through regulation of nitric oxide and adenosine monophosphate activated protein kinase/mammalian target of rapamycin signaling pathway. Environ. Toxicol. 37, 2503–2514. doi:10.1002/tox.23613.
Chen, L., Qi, M., Zhang, L., Yu, F., Tao, D., Xu, C, 2023. Di(2-ethylhexyl) phthalate and microplastics cause necroptosis and apoptosis in hepatocytes of mice by inducing oxidative stress. Environ. Toxicol. 38, 1226–1238. doi:10.1002/tox.23759.
Chen, L., Tao, D., Yu, F., Wang, T., Qi, M., Xu, S, 2022b. Cineole regulates Wnt/β-catenin pathway through Nrf2/keap1/ROS to inhibit bisphenol A-induced apoptosis, autophagy inhibition and immunosuppression of grass carp hepatocytes. Fish Shellfish Immunol. 131, 30–41. doi:10.1016/j.fsi.2022.09.067.
Dagher, J.B., Hahn-Townsend, C.K., Kaimal, A., Mansi, M.A., Henriquez, J.E., Tran, D.G., et al., 2021. Independent and combined effects of bisphenol A and Diethylhexyl phthalate on gestational outcomes and offspring development in sprague-dawley rats. Chemosphere 263, 128307. doi:10.1016/j.chemosphere.2020.128307.
Geethika, M., Singh, N., Kumar, S., Kumar, S.K.N., Mugesh, G., 2023. A redox modulatory sod mimetic nanozyme prevents the formation of cytotoxic peroxynitrite and improves nitric oxide bioavailability in human endothelial cells. Adv. Healthc. Mater., e2300621 doi:10.1002/adhm.202300621.
Graziani, N.S., Carreras, H., Wannaz, E., 2019. Atmospheric levels of BPA associated with particulate matter in an urban environment. Heliyon. 5, e01419. https://pmc/articles/PMC6454204/.
Guo, G., Yang, W., Sun, C., Wang, X., 2023. Dissecting the Potential Role of Ferroptosis in Liver Diseases: An Updated Review. Free Radical Research, pp. 1–12.
Ha, H.C., Snyder, S.H., 1999. Poly(ADP-ribose) polymerase is A mediator of necrotic cell death by ATP depletion. Proc. Natl. Acad. Sci. U.S.A. 96, 13978–13982. https://pmc/articles/PMC24176/.
Han, D., Yao, Y., Chen, L., Miao, Z., Xu, S., 2022. Apigenin ameliorates Di(2-ethylhexyl) phthalate-induced ferroptosis: the activation of glutathione peroxidase 4 and suppression of iron intake. Food Chem. Toxicol. 164, 113089. https://article/pii/S0278691522002873.
Lan, T., Wang, W., Zeng, X.X., Tong, Y.H., Mao, Z.J., Wang, S.W., 2023. Saikosaponin A triggers cell ferroptosis in hepatocellular carcinoma by inducing endoplasmic reticulum stress-stimulated ATF3 expression. Biochem. Biophys. Res. Commun. 674, 10–18. https://article/pii/S0006291X23008410.
Lei, Y., Xu, T., Sun, W., Wang, X., Gao, M., Lin, H., 2023. Evodiamine alleviates DEHP-induced hepatocyte pyroptosis, necroptosis and immunosuppression in grass CarpThrough ROS-regulated TLR4 /MyD88 / NF-κB pathway. Fish Shellfish Immunol. 140, 108995. https://.gov/37573970/.
Li, Q., Chen, G., Wang, W., Zhang, W., Ding, Y., Zhao, T, 2018. A novel Se-polysaccharide from Se-enriched G. Frondosa protects against immunosuppression and low Se status in Se-deficient mice. Int. J. Biol. Macromol. 117, 878–889. doi:10.1016/j.ijbiomac.2018.05.180.
Li, X., Bai, Y., Bi, Y., Wu, Q., Xu, S., 2023. Baicalin suppressed necroptosis and inflammation against chlorpyrifos toxicity; involving in ER stress and oxidative stress in carp gills. Fish Shellfish Immunol. 139, 108883. doi:10.1016/j.fsi.2023.108883.
Li, X., Wu, Q., Chen, D., Bai, Y., Yang, Y., Xu, S., 2024. Environment-relevant concentrations of cadmium induces necroptosis and inflammation; baicalein maintains gill homeostasis through suppressing ROS/ER stress signaling in common carps (Cyprinus carpio L.). Environ. Pollut. 340, 122805. https://pubmed.gov/37913980/.
Liu, G., Sun, W., Wang, F., Jia, G., Zhao, H., Chen, X., 2023a. Dietary tryptophan supplementation enhances mitochondrial function and reduces pyroptosis in the spleen and thymus of piglets after lipopolysaccharide challenge. Animal: Int. J. Anim. Biosci. 17, 100714. doi:10.1016/j.animal.2023.100714.
Liu, J., Chen, T., Wang, S., Wu, H., Xu, S., 2022. BPA exposure aggravates necroptosis of myocardial tissue in selenium deficient broilers through NO-dependent endoplasmic reticulum stress. Toxicology. 472, 153190. doi:10.1016/j.tox.2022.153190.
Liu, Y., Yin, S., He, Y., Tang, J., Pu, J., Jia, G., et al., 2023b. Hydroxy-selenomethionine mitigated chronic heat stress-induced porcine splenic damage via activation of Nrf2/Keap1 signal and suppression of NF-κb and STAT signal. Int. J. Mol. Sci. 24. https://pmc/articles/PMC10094443/.
Lv, X., Ren, M., Xu, T., Gao, M., Liu, H., Lin, H., 2023. Selenium alleviates lead-induced CIK cells Pyroptosis and inflammation through IRAK1/TAK1/IKK pathway. Fish Shellfish Immunol. 142, 109101. https://pubmed.ncbi.nlm.nih.gov/37758100/.
Ma, J., Wang, J., Ma, C., Cai, Q., Wu, S., Hu, W, 2023. Wnt5a/Ca(2+) signaling regulates silica-induced Ferroptosis in mouse macrophages by altering ER stress-mediated redox balance. Toxicology. 490, 153514. doi:10.1016/j.tox.2023.153514.
Mir, H., Rajawat, J., Vohra, I., Vaishnav, J., Kadam, A., Begum, R., 2020. Signaling interplay between PARP1 and ROS regulates stress-induced cell death and developmental changes in dictyostelium discoideum. Exp. Cell Res. 397, 112364. doi:10.1016/j.yexcr.2020.112364.
Mocchegiani, E., Corradi, A., Santarelli, L., Tibaldi, A., DeAngelis, E., Borghetti, P, 1998. Zinc, thymic endocrine activity and mitogen responsiveness (PHA) in piglets exposed to maternal aflatoxicosis B1 and G1. Vet. Immunol. Immunopathol. 62, 245–260. doi:10.1016/S0165-2427(98)00073-7.
Noonan, G.O., Ackerman, L.K., Begley, T.H., 2011. Concentration of bisphenol A in highly consumed canned foods on the U.S. market. J. Agric. Food Chem. 59, 7178–7185. doi:10.1021/jf201076f.
Park, S.J., Jang, J.W., Moon, E.Y., 2023. Bisphenol A-induced autophagy ameliorates human B cell death through Nrf2-mediated regulation of Atg7 and Beclin1 expression By Syk activation. Ecotoxicol. Environ. Saf. 260, 115061. doi:10.1016/j.ecoenv.2023.115061.
Peng, X., Cui, H., Yuan, J., Cui, W., Fang, J., Zuo, Z, 2011. Low-selenium diet induces cell cycle arrest of thymocytes and alters serum IL-2 content in chickens. Biol. Trace Elem. Res. 144, 688–694. https://article/10.1007/s12011-011-9077-y.
Pu, F., Chen, F., Zhang, Z., Shi, D., Zhong, B., Lv, X., et al., 2022. Ferroptosis as A novel form of regulated cell death: implications in the pathogenesis, Oncometabolism and treatment of human cancer. Genes Dis. 9, 347–357. https://pubmed.gov/35224151/.
Qian, Q., Song, J., Pu, Q., Chen, C., Yan, J., Wang, H., 2023. Acute/Chronic exposure to bisphenol A induced

immunotoxicity in Zebrafish and its potential association with pancreatic cancer risk. Aquat. Toxicol. 258, 106514. https://pmc/articles/PMC8843993/.

Qiu, J., Zhou, P., Shen, X., 2022. Effects of Se-yeast on immune and antioxidant in the Se-deprived Pishan red sheep. Biol. Trace Elem. Res. 200, 2741–2749. doi:10.1016/j.aquatox.2023.106514.

Rochester, J.R., 2013. Bisphenol A and human health: a review of the literature. Reprod. Toxicol. 42, 132–155. https://gov/17164221/.

Sabry, R., Williams, M., LaMarre, J., Favetta, L.A., 2023. Granulosa cells undergo BPA-induced apoptosis in A MiR-21-independent manner. Exp. Cell Res. 427, 113574. doi:10.1016/j.intimp.2023.110371.

Sajiki, J., Miyamoto, F., Fukata, H., Mori, C., Yonekubo, J., Hayakawa, K., 2007. Bisphenol A (BPA) and its source in foods in Japanese markets. Food Addit. Contam. 24, 103–112. doi:10.1016/j.jhazmat.2021.126172.

Shi, Q., Qian, Y., Wang, B., Liu, L., Chen, Y., Chen, C., et al., 2023. Glycyrrhizin protects against particulate matter-induced lung injury via regulation of endoplasmic reticulum stress and NLRP3 inflammasome-mediated pyroptosis through Nrf2/HO-1/NQO1 signaling pathway. Int. Immunopharmacol. 120, 110371. doi:10.1016/j.intimp.2023.110371.

Song, N., Li, X., Cui, Y., Zhang, T., Xu, S., Li, S., 2021. Hydrogen sulfide exposure induces pyroptosis in the trachea of broilers via the regulatory effect of CircRNA-17828/miR-6631-5p/DUSP6 crosstalk on ROS production. J. Hazard. Mater. 418, 126172. doi:10.1016/j.jhazmat.2021.126172.

Tripathi, A., Kalita, J., Kant, S., Misra, U.K., 2022. Oxidative stress and ER stress are related to severity of tubercular infection. Microb. Pathog. 172, 105764. doi:10.1016/j.micpath.2022.105764.

Wang, B., Cui, Y., Zhang, Q., Wang, S., Xu, S., 2021. Selenomethionine alleviates LPS-induced JNK/NLRP3 inflammasome-dependent necroptosis by modulating MiR-15a and oxidative stress in chicken lungs. Metallomics: Integrat. Biometal. Sci. 13. https://gov/34329475/.

Wang, J., Yin, Y., Zhang, Q., Deng, X., Miao, Z., Xu, S., 2023a. HgCl(2) exposure mediates Pyroptosis Of HD11 cells and promotes M1 polarization and the release of inflammatory factors through ROS/Nrf2/NLRP3. Ecotoxicol. Environ. Saf. 269, 115779. https://PMC8844831/?report=reader.

Wang, K., Liu, H., Sun, W., Guo, J., Jiang, Z., Xu, S., et al., 2023b. Eucalyptol alleviates avermectin exposure-induced apoptosis and necroptosis of grass carp hepatocytes by regulating ROS/NLRP3 axis. Aquatic Toxicol. 264, 106739. https://pubmed.gov/37918148/.

Wang, S., Zhao, X., Liu, Q., Wang, Y., Li, S., Xu, S., 2022a. Selenoprotein K protects skeletal muscle from damage and is required for satellite cells-mediated myogenic differentiation. Redox Biol. 50, 102255. https://pubmed.gov/35144051/.

Wang, Y., Liu, X., Jing, H., Ren, H., Xu, S., Guo, M, 2022b. Trimethyltin induces apoptosis and necroptosis of mouse liver by oxidative stress through YAP phosphorylation. Ecotoxicol. Environ. Saf. 248, 114327. doi:10.1016/j.ecoenv.2022.114327.

Xia, B., Li, Q., Zheng, K., Wu, J., Huang, C., Liu, K., et al., 2023. Down-regulation of Hrd1 protects against myocardial ischemia-reperfusion injury by regulating PPARα to prevent oxidative stress, endoplasmic reticulum stress, and cellular apoptosis. Eur. J. Pharmacol. 954, 175864. doi:10.1016/j.ejphar.2023.175864.

Xiao, Y., Huang, Q., Zheng, Z., Ma, H., 2021. Selenium release kinetics and mechanism from cordyceps sinensis exopolysaccharide-selenium composite nanoparticles in simulated gastrointestinal conditions. Food Chem 350, 129223. doi:10.1016/j.foodchem.2021.129223.

Yang, L., Qi, M., Du, X., Xia, Z., Fu, G., Chen, X., 2022. Selenium concentration is associated with occurrence and diagnosis of three cardiovascular diseases: a systematic review and meta-analysis. J. Trace Element. Med. Biol.: Organ Soc. Mineral. Trace Element. (GMS) 70, 126908. doi:10.1016/j.jtemb.2021.126908.

Ye, Z., Zhang, F., Wang, P., Ran, Y., Liu, C., Lu, J., 2023. Baicalein relieves brain injury via inhibiting ferroptosis and endoplasmic reticulum stress in a rat model of cardiac arrest. Shock 59, 434–441. https://abstract/2023/03000/baicalein_relieves_brain_injury_via_.

Yoshida, T., Horie, M., Hoshino, Y., Nakazawa, H., 2001. Determination of bisphenol A in canned vegetables and fruit by high performance liquid chromatography. Food Addit. Contam. 18, 69–75. https://pubmed.ncbi.nlm.nih.gov/11212549/.

Zhang, H., Sun, K., Gao, M., Xu, S., 2023. Zinc inhibits lead-induced oxidative stress and apoptosis of ST cells through ROS/PTEN/PI3K/AKT Axis. Biol. Trace Elem. Res. https://article/10.1007/s12011-023-03721-0.

Zhang, W., Yin, K., Shi, J., Shi, X., Qi, X., Lin, H., 2022. The decrease of Selenoprotein K induced by selenium deficiency in diet improves apoptosis and cell progression block in chicken liver Via the PTEN/PI3K/AKT pathway. Free Radic. Biol. Med. 189, 20–31. https://pubmed.ncbi.nlm.nih.gov/35841984/.

Zhang, J.Y., Wang, S.C., Hao, X.F., Sun, G., Xu, S.W., 2020. The antagonistic effect of selenium on lead-induced necroptosis Via MAPK/NF-κB pathway and HSPs activation in the chicken spleen. Ecotoxicol. Environ. Saf. 204, 111049. doi:10.1016/j.ecoenv.2020.111049.

Zhang, Z.W., Wang, Q.H., Zhang, J.L., L, i S., Wang, X.L., Xu, S.W., 2012. Effects of oxidative stress on immunosuppression induced by selenium deficiency in chickens. Biol. Trace Elem. Res. 149, 352–361. https://article/10.1007/s12011-012-9439-0.

Zhou, X., Cao, N., Xu, D., Tian, Y., Shen, X., Jiang, D., et al., 2022. Polysaccharide of atractylodes macrocephala Koidz alleviates cyclophosphamide-induced thymus ferroptosis in gosling. Animals: Open Access J. MDPI 12. https://pmc/articles/PMC9738654/.

Zhu, H., Gao, M., Sun, W., Liu, H., Xu, S., Li, X., 2023. ROS/ER stress contributes to Trimethyltin chloride-mediated hepatotoxicity; tea polyphenols alleviate apoptosis and immunosuppression. Comparat. Biochem. Physiol. Toxicol. Pharmacol.: CBP 263, 109505. doi:10.1016/j.cbpc.2022.109505.